



Single and Three Phases Sensitive Load Compensation by Electric Spring Using Proportional-Resonant and Repetitive Controllers

Mehrdad Mohammadzadeh^{a,*}, Abbas Ketabi^b

^{a,b}Department of Electrical and Computer Engineering, Kashan university, Kashan, Iran

Received: 2021-02-26

Accepted: 2021-04-24

Abstract

Electric springs (ES) are often known to be demand-side power management systems in decentralized grids with renewable energy sources, which, due to their nature, inject unreliable electricity power into the system.

The second type of electrical spring (ES_2) produces an intelligent load by placing it next to a sensitive load, which, in addition to regulating the voltage level, will optimize various parameters of the power quality for the sensitive load.

In imbalance grids with harmonic voltages and local non-linear load, where conventional controllers are used, the intelligent load cannot improve the power quality for a sensitive load.

In this paper, a proportional resonance (PR) controller is used to regulate both the voltage level and the source voltage imbalances due to the least tracking error in the sinusoidal mode as well as a repetitive controller (RC) is designed to reduce THD and improve the power factor thanks to its infinite poles on the imaginary axis. Finally, these two suggested controllers were tested simultaneously in three-phase and single-phase grids by mathematical and machine simulation.

The grid considered in this paper has harmonics up to order 17 and voltage fluctuations in the range of 0.954 to 1.1 per unit, as well as a local non-linear load with 100% of the sensitive load size and, in the three-phase mode, the grid, has unbalanced three-phase load.

The results of the MATLAB simulation for electrical spring, controlled by the PR RC controller, which is a combination of two proportional resonance controllers and a repetitive controller in both three and single-phase mode. Note that the sensitive load voltage is completely adjusted to its reference value, THD reduces by 80.31% compared to the uncompensated condition and will be less than the value defined by the IEEE standard and the power factor rises up to near the unit.

Keywords: Electric spring, Proportional-Resonant controller, Repetitive controller, Sensitive load, Power quality.

1. Introduction

The application of clean energies such as solar and wind energy is expanding due to their environmental benefits. Nevertheless, renewable energies production is erratic and unreliable, causing

it impossible to forecast the generation of electricity [1]. Variability of production power together with the inability to predict output power causes voltage fluctuation in the grid that are not acceptable for sensitive loads. On the other hand, due to the local

non-linear loads, harmonics are created at the grid current and voltage[2]–[5]. Electric springs were first introduced in smart grids for voltage regulation at the load side in 2012 [2], where for the first time the grid loads were divided into the two types of sensitive and non-sensitive [6]. Electric spring with the help of a power electronic converter can regulate sensitive load voltage through the control voltage and power of the non-sensitive load. The electric spring is divided into the two categories based on the structure:

1-The first type of electric spring uses a capacitor in the DC link, which is only able to compensate voltage level and reactive power [2]–[7].

2-type two electric spring, with a structure similar to the first type with the difference that instead of using a capacitor in the DC link, energy storage source is used such as batteries and/or voltage source[2], [6].

A result of these changes done in the structure of ES-I, the second type electric spring, in addition to the mentioned benefits for the first type of electric spring, Allowing electric spring to control either reactive and active power [7], [8].

To control the electric springs, some methods are presented, each with special advantages and disadvantages. In most electric spring control methods, the main purpose of the method is to bring the voltage to the desired level and in some cases also to increase the power factor. In [1], [6], [17], [18], [9]–[16] the method of compensating with the optimal values is investigated, no method was proposed to compensate for the harmonics of the grid voltage and the negative effects of local nonlinear load.

In Table 1, the available related research works are divided based on the type of controller, the reference voltage determination method, and the power quality issues. In the classification by type of controller, most of the methods have been focused on the PI controller and just a few of them using PR controller. In classification based on the method of reference voltage estimation, various ideas have been proposed, one of the most effective ways of calculating the reference voltage is the MCV method. In the segmentation focused on issues of power quality, most articles concentrate on the regulation of voltage level (VR) and enhancement of the power factor (PF).

In order to address the weaknesses of the previous research, this paper suggests an improved control method for ES-2 called PR_RC, which increase the quality of the voltage waveform as well as the grid current waveform with just a quick and easy control

system. The suggested control system is a mixture of a proportional_Resonant controller and a repetitive controller. Since the grid under study in this article has voltage fluctuations, and also in the case of three phases, it is considered to have an unbalanced three phase load; The proportional resonance (PR) controller is used to regulate both the voltage level and the source voltage imbalances due to the least tracking error in the sinusoidal mode. Also, due to the grid voltage harmonics up to order 17 and non-linear local loads that caused power quality issues, in the grid under-analyzed, power quality has to be optimized for the sensitive load, And considering that the previous control methods have not offered a solution to the problems of power quality in this situation in this paper a repetitive controller (RC) is designed to reduce THD and improve the power factor thanks to its infinite poles on the imaginary axis. The effectiveness of the designed control system is analyzed through mathematical modeling and MATLAB simulation.

TABLE 1. Summary of the Literature Review in the Research Field of Electric spring control

Reference	Controller	reference voltage	Improve power quality
[6]	PI	Power control	VR
[10]	PI	Droop control	VR+PF
[14]	PI	Power control	VR+PF
[15]	PI+PR	δ control	VR+PF
[13]	PI	RCD	VR+PF
[8]	PI	dq decoupling	VR+PF
[16]	PI	SPD	VR+PF
[9]	PI	Instantaneous power theory	VR+PF
[11]	PI	OCC	VR+PF
[12]	PR	MCV	VR+PF
[7]	PI+PR	Grid-tied power control	VR+PF
[17]	PI	AC PI	VR+PF
[18]	PI	Power decoupling control	VR+PF+THD
[1]	PI+PR	Decoupled power	VR+PF

Reference	Controller	reference voltage	Improve power quality
		control	

This article is structured in the following manner. Initial notions are discussed in chapter two. the proportional_resonance controller equations are created and discussed in Chapter Three. In chapter four, it is presented the designed controller for harmonics compensations. In chapter five different situation Simulation are discussed and results are presented.

2. OPERATION PRINCIPLE AND PROBLEM FORMULATION

As described in the previous section; the typical structure of the electric spring second type is shown in Fig. 1 as can be seen in Fig. 1 the decentralized renewable electricity site is linked to the electricity grid. The ES is integrated into the system to restrict the voltage fluctuations caused by wind and solar power.

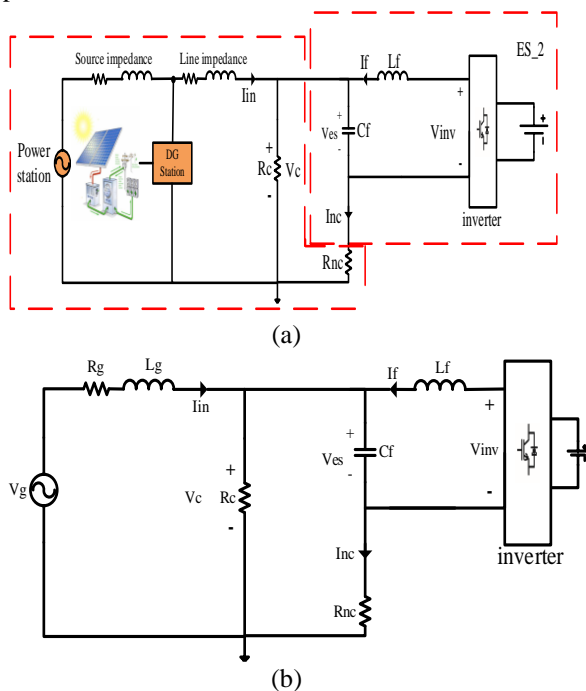


Figure 1. (a)Electric spring schematic
(b)equivalent circuit

The electric spring is marked in the dotted box. The capacitor used as the filter (Cf) will play the role of a controllable voltage source and This voltage is changed by the inverter control signal.

Considering state and input variables as follows:

$$X = \begin{bmatrix} I_{inv} & I_f & V_{es} \end{bmatrix}^T \quad (1)$$

$$U = \begin{bmatrix} V_g & V_{inv} \end{bmatrix}^T \quad (2)$$

$$Y = V_c \quad (3)$$

In Fig. 1 Kirchoff's law can be written as:

$$KCL: I_{inv} = I_{nc} + \frac{V_c}{Z_c} \quad (4)$$

$$KVL: V_{es} + L_f \frac{di_f}{dt} = V_{inv} \quad (5)$$

$$KVL: R_g I_{inv} + L_g \frac{di_{inv}}{dt} + V_c = V_g \quad (6)$$

$$KCL: I_{nc} + I_f = C_f \frac{dV_{es}}{dt} \quad (7)$$

$$KVL: V_{es} + Z_{nc} I_{nc} = V_c \quad (8)$$

From (5) and (6) the following equations are obtained:

$$\frac{di_f}{dt} = \frac{-V_{es}}{L_f} + \frac{V_{inv}}{L_f} \quad (9)$$

$$\frac{di_{inv}}{dt} = \frac{V_g}{L_g} - \frac{R_g}{L_g} I_{inv} - \frac{V_c}{L_g} \quad (10)$$

Where L_f is the output filter inductance and I_f is the current of the filter L_g and R_g is the equivalent inductance and resistance of the transmission line, respectively.

The Inverter current equation is calculating from (4) and (8):

$$I_{inv} = I_{nc} + \frac{V_{es} + Z_{nc} I_{nc}}{Z_c} \quad (11)$$

Where Z_{nc} and Z_c are noncritical and critical load, respectively.

$$I_{nc} \left(1 + \frac{Z_{nc}}{Z_c} \right) = I_{inv} - \frac{V_{es}}{Z_c} \quad (12)$$

$$I_{nc} = \frac{I_{inv}}{\left(1 + \frac{Z_{nc}}{Z_c} \right)} - \frac{V_{es}}{(Z_c + Z_{nc})} \quad (13)$$

From (8) and (13) critical load voltage can be written as:

$$V_c = V_{es} + Z_{nc} \left(\frac{I_{inv}}{\left(1 + \frac{Z_{nc}}{Z_c}\right)} - \frac{V_{es}}{(Z_c + Z_{nc})} \right) \quad (14)$$

$$V_c = I_{inv} \left(\frac{Z_{nc}}{\left(1 + \frac{Z_{nc}}{Z_c}\right)} \right) + V_{es} \left(1 - \frac{Z_{nc}}{(Z_c + Z_{nc})} \right) \quad (15)$$

From (7) and (13) follow equation is derived as:

$$\frac{dV_{es}}{dt} = \frac{I_f}{C_f} + \frac{I_{inv}}{C_f + \frac{Z_{nc}}{Z_c} I_f} - \frac{V_{es}}{C_f (Z_c + Z_{nc})} \quad (16)$$

By solving (10) and (15) it can be obtained:

$$\frac{di_{inv}}{dt} = \frac{V_g}{L_g} - \frac{R_g}{L_g} I_{inv} - \frac{1}{L_g} \left(\frac{Z_{nc}}{\left(1 + \frac{Z_{nc}}{Z_c}\right)} \right) I_{inv} - V_{es} \left(1 - \frac{Z_{nc}}{(Z_c + Z_{nc})} \right) \frac{1}{L_g} \quad (17)$$

Finally, according to the (9), (15), (16) and (17), the equation of steady-state can be expressed as:

$$\begin{bmatrix} \frac{di_{inv}}{dt} \\ \frac{di_f}{dt} \\ \frac{dV_{es}}{dt} \end{bmatrix} = \begin{bmatrix} -\frac{R_g}{L_g} - \frac{1}{L_g} \left(\frac{Z_{nc}}{\left(1 + \frac{Z_{nc}}{Z_c}\right)} \right) & 0 & -\left(1 - \frac{Z_{nc}}{(Z_c + Z_{nc})} \right) \frac{1}{L_g} \\ 0 & 0 & -\frac{1}{L_f} \\ \frac{1}{C_f + C_f \frac{Z_{nc}}{Z_c}} & \frac{1}{C_f} & -\frac{1}{C_f (Z_c + Z_{nc})} \end{bmatrix} \begin{bmatrix} I_{inv} \\ I_f \\ V_{es} \end{bmatrix} + \begin{bmatrix} \frac{1}{L_g} & 0 \\ 0 & \frac{1}{L_f} \\ 0 & 0 \end{bmatrix} \begin{bmatrix} V_g \\ V_{inv} \end{bmatrix} \quad (18)$$

$$Y = \begin{bmatrix} \left(\frac{Z_{nc}}{\left(1 + \frac{Z_{nc}}{Z_c}\right)} \right) & 0 \\ 0 & \left(\frac{1 - Z_{nc}}{(Z_c + Z_{nc})} \right) \end{bmatrix} \quad (19)$$

$$D = 0 \quad (20)$$

3. DESIGNING CONTROL SYSTEM FOR VOLTAGE REGULATION

The proportional resonant control system is designed to create the minimum voltage fluctuations between the sensitive load voltage and the reference voltage. To achieve this purpose, the PR controller is used in this paper because it has the least persistent error in the sinusoidal input mode[19].

The PR controller transfer function is ideally as follows: $G(s) = K_p + \frac{K_R s}{s^2 + \omega_s^2}$

$$(21)$$

The optimal PR control system has unlimited amplification at the resonance frequency and zero phase change throughout all other frequencies. Due to the infinity gain of this controller, there is a possibility of system stability issues (if the error becomes large between the reference and the measured signal); As a result, to improve system stability, the PR transfer function modified by attaching the damping component to the ideal form of this equation. the non-ideal form of the proportional resonant controller is as follow:

$$G_2(s) = K_p + k_R \times \frac{\omega_c \times s + \omega_c}{s^2 + 2\omega_c + \omega_s^2} \quad (22)$$

ω_c has a range in the ac frequency range ω_s . The gain in the resonant frequency is reduced by the improvements made to this function, such that the stability issue is resolved.

3.1. Determination of the controller bandwidth:

Through the bode diagram, the impact of bandwidth on the performance of this controller can be seen in Fig. 2.

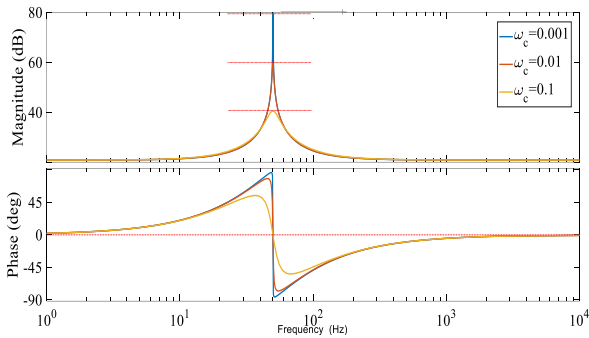


Figure 2. PR controller bode diagram for different ω_c

Fig.2 Displays the bode diagram of the proportional resonant control system for various ω_c values. According to the magnitude and phase shift and cut off frequency of this diagram ω_c chooses equal to 6.2832 for better results.

3.2. Determination of the controller gain K_p and K_R :

In this paper GENSS (Generalized State-Space) model is used to optimize PR controller parameters. When a tunable GENSS model of a control system Available then optimization of controller parameters can be done through the intelligent algorithms (genetic, neural, neural fuzzy). The PR optimization method achieved these goals by adjusting the PR gains to strike a reasonable compromise between efficiency and reliability.

Another way to Select the coefficients is to use the bode diagram. In the bode diagram plotted in Fig. 3, concerning the choice of different k_p values, it can be seen that the gain of the controller does not change much, at the same time with increasing k_p the system bandwidth narrows and the filter performance improves.

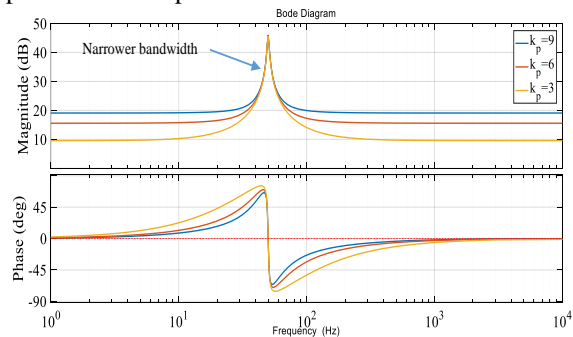


Figure 3. Non-ideal PR controller bode diagram with a different value of k_p

At the same time to select the coefficient k_R , the system dynamic response is considered and the k_R value is determined on the basis of the speed of response required.

Finally, to select the optimal coefficients the phase margin and gain margin information was considered in the MATLAB SISOTOOL. For cut off frequency equal to 6.2832 the optimal coefficient is 11.195.

4. DESIGNING CONTROLLER FOR HARMONICS COMPENSATIONS

Typically, in the power grid, there are exist harmonics with various amplitudes and orders for several reasons and also if a local nonlinear load is present or a sensitive load itself is a nonlinear load, these instances may create a number of power issues that usual control systems will not be able to compensate for these problems and prevent their effects on sensitive load voltage; In the present paper, the theory of the internal model is being used for harmonic elimination; On the basis of this theory, to follow the reference signal or remove the input perturbations, the closed-loop transfer function Must be included the reference signal transfer function or the input perturbation transfer function[20]–[22]for example: See the following signals and their transfer functions needed for compensating them:

$$U(s) \text{ (Step signal)} \rightarrow I : \frac{1}{s} \rightarrow \text{PI controller} \quad (23)$$

$$U(s) \text{ (Sinusoidal signal)} \rightarrow R : \frac{K_i}{s^2 + \omega^2} \rightarrow \text{PR controller} \quad (24)$$

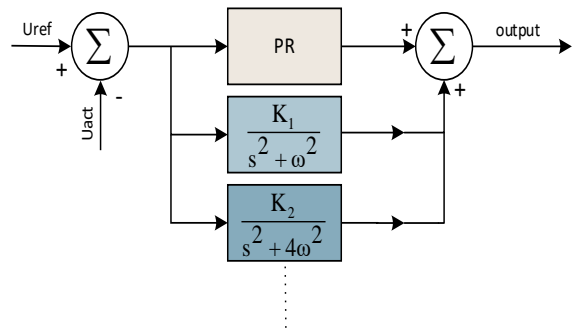


Figure 3. Basic internal model control block diagram As a result, to eliminate harmonic perturbations, the closed-loop transfer function must include

$$\frac{K_i}{s^2 + (h\omega)^2} \text{ terms. Where poles in each harmonic}$$

transfer functions are equal to: $S = \pm jh\omega$. Fig. 4 displays a schematic of transfer function is required to compensate for several harmonics. As can be

seen, each harmonic needs to be modeled independently. Using this control method requires that all harmonics be individually modeled and included in the closed-loop transfer function. To simplify and solve this problem, a Repetitive Controller is introduced. The flexible time-delay method will produce any periodic signal with the T_s cycle. This transfer function will produce an unlimited number of poles on an imaginary axis. This huge number of poles will be made because of the delay in the time.

The simple RC transfer function is as follows[23]:

$$G(s) = \frac{W(s)e^{-\tau_d s}}{1 - W(s)e^{-\tau_d s}} \quad (25)$$

where $e^{-\tau_d s}$ Indicates the delay of one cycle

and $W(s) = \frac{\omega_c}{s + \omega_c}$ is low pass filter.

$$\text{For } \tau = \tau_d + \frac{1}{\omega_c} \text{ and } \frac{1}{\omega_c} \ll 1 \rightarrow \tau_d = \tau = \frac{1}{f_1} \quad (26)$$

$$S_h = j \frac{2\pi}{\tau} h \quad (27)$$

The block diagram of equation 25 is shown in Fig.5:

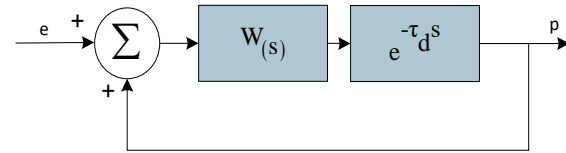


Figure 4. Basic RC controller block diagram

Because digital devices are more flexible than analog devices and have a cheaper price as well as higher processing speeds, this article uses a digital RC control structure.

The transfer function of the controller used in this paper is as follows:

$$G_{RC}(z) = \frac{K_r z^k z^{-N}}{1 - Q(z) z^{-N}} \quad (28)$$

It is used to compensate harmonics produced on the load and the grid side.

Where $N = \frac{f_{sample}}{f_s}$ the number of delays is in the sample [21].

4.1. options for filter $Q(z)$:

rising the peak gain of the Repetitive Controller in the high-frequency region caused device reliability is enhanced. According to the mentioned case, $Q(z)$ filter is used for this purpose. Typically, the

selection of filters in most cases is done experimentally and through the simulation.

The selection of filters from the following two methods is examined and simulated in this paper:

- 1: A value close to one $Q(z) = 0.95$
- 2: A low pass filter $Q(z) = (Z + 2 + Z^{-1}) / 4$ (29)

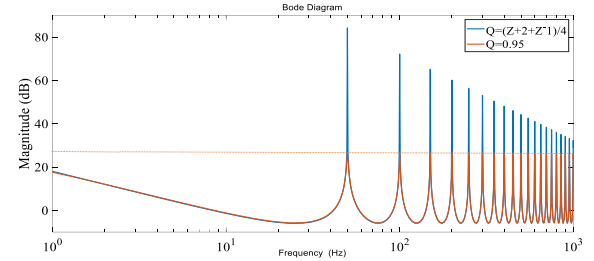


Figure 5. Bode diagram of the open-loop transfer function of controller with $Q(z) = 0.95$ (red) and $Q(z) = (Z + 2 + Z^{-1}) / 4$ (blue)

The first type of filter cannot be a good choice due to having a constant gain for all frequencies. Since the designed low-pass filter has the maximum gain in the low-frequency range and the lowest gain in the high-frequency range based on Fig. 6, so it can be a good choice.

4.2. Pick the best phase shift Compensator:

Due to the internal structure of the system $_{LC}$ filter_, which acts as an LPF and causes some phase-lag in the system and to compensate for the effect of this filter, the phase lag must be compensated by a phase lead generating factor such as Z^k . Fig. 7 presents the Bode diagram with different values of k . Z^k causes phase to be constant at low-frequency values, and phase change occurs at higher frequency values.

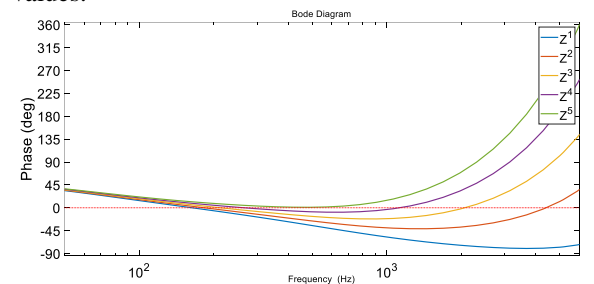


Figure 7. Frequency characteristic of the system in different lead links Z^k

According to the description given and Due to the behavior of phase diagram if the value of Z be considered to 4 in the desired frequency range (about 10 to 1000), the value of this coefficient is finally selected equal to 4.

4.3. Pick the best controller gain:

The amplitude-frequency diagram of the system is analyzed to choose the most suitable coefficient K_r . According to Fig. 8, if the magnitude of K_r increases, the frequency response shifts as well.

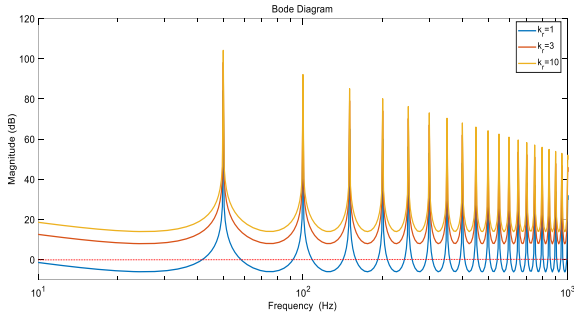


Figure 8. Determine of controller gain K_r

Fig. 8 displays the frequency response of the controller for the various values of K_r . If the values below 3 are chosen for K_r , the gain range of the controller would be so limited that it will no longer be able to compensate for the harmonics at a steady state condition. So, the best peak gain for harmonics compensation chooses (base on harmonics order that we want to compensate) through the bode diagram. In this paper based on the situation, which source voltage has standard harmonics up to order 17, and nonlinear load parallel to sensitive load and source voltage amplitude is not constant k_r is Set to 6. The reference voltage of electric spring, U_{ref} , is determined by minimum compensating voltage (MCV) method[12].

Finally, according to the explanations given for the Repetitive controllers the following block diagram is drawn in Fig. 9.

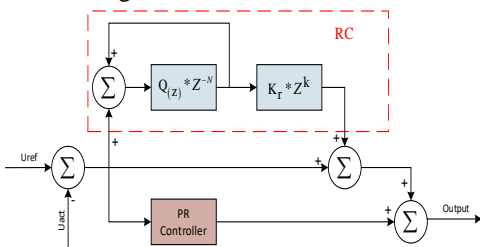


Figure 6. Proposed PR_RC controller block diagram

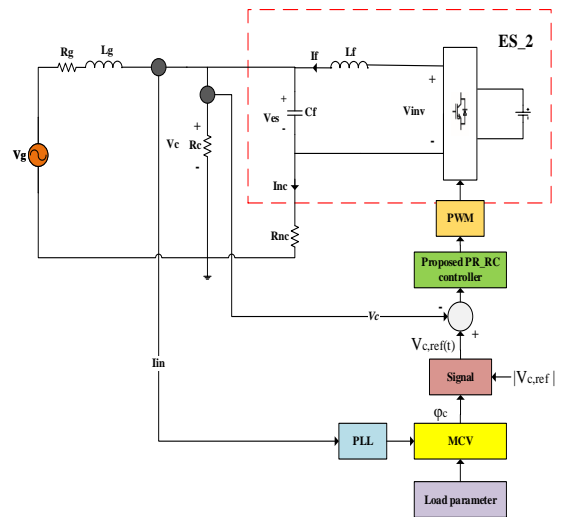


Figure 7. System block diagram of PR-controlled ES-2

5. SIMULATION

MATLAB software was used to simulate and evaluate the efficiency of the proposed controller in this paper. To simulate this circuit, two case study with six scenarios is checked out.

- Scenario A)** Single-phase grid, with source voltage harmonics and local nonlinear load without any controller
- Scenario B)** Single-phase grid, without source voltage harmonics and local nonlinear load with PR controller
- Scenario C)** Single-phase grid, with source voltage harmonics and without local nonlinear load with PR controller
- Scenario D)** Single-phase grid, with source voltage harmonics and local nonlinear load with PR controller
- Scenario E)** Single-phase grid, with source voltage harmonics and local nonlinear load with PR_RC controller
- Scenario F)** Three-phase grid, with source voltage harmonics and local nonlinear load

The task of the control system is to approach the voltage waveform to the sine wave state and bring the voltage amplitude to the value of 311 volt. The controller should also improve the quality of the THD.

TABLE 2. Simulated test system parameters

symbol	Description	Value
Zc	Critical linear load impedance	8 Ω
Znc	Noncritical linear load impedance	8 Ω
Zg	Transmission line impedance	0.1 + jω2.4e-3
Vdc	DC-link voltage	800 V
Vref	Reference	220 VRMS
Fsw	Switching frequency	20 KHz
Fs	Sampling frequency	10 KHz
Fg	Grid frequency	50 Hz
Zdc	Load of diode rectifier	R=15 Ω C=2200μF
Lf	Output filter inductance	26e-4 H
Cf	Output filter capacitance	3e-6 F

5.1. Single Phase Load

CASE ONE, SCENARIO A

For the first test, the sensitive load in the grid has been exposed to voltage fluctuations and source voltage harmonics without any compensation. In addition to the voltage fluctuations, non-linear loads parallel to the sensitive load have caused voltage THD increase in the sensitive load side. Fig. 11,12,13 represent the source voltage, sensitive load voltage and current characteristic of the local nonlinear load, respectively.

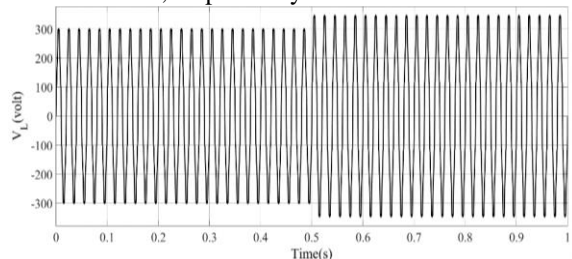
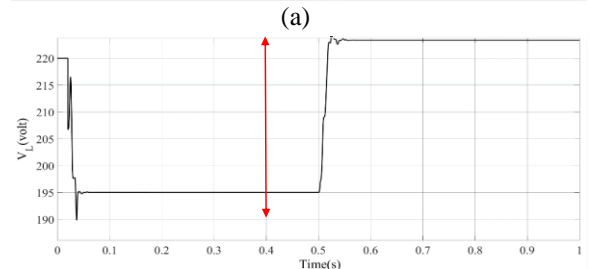
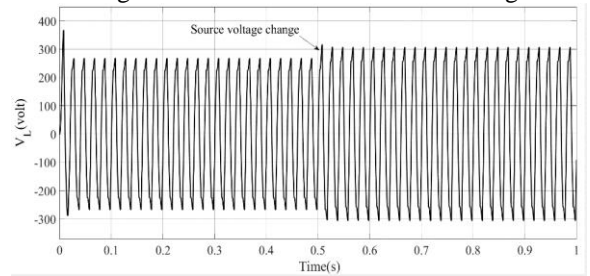
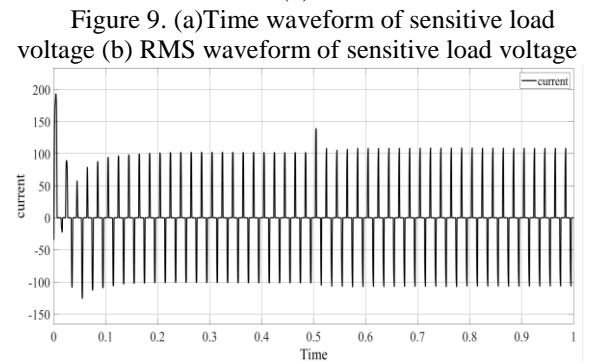


Figure 8. Time waveform source voltage



(a)



(b)

Figure 9. (a)Time waveform of sensitive load voltage (b) RMS waveform of sensitive load voltage

As can be seen in Fig. 11 in second 0.5 voltage amplitude changes from 0.954p.u to 1.1p.u. As can be seen from Fig.12 the sensitive load voltage changes with the source voltage change and the sensitive load is not capable of operating in its nominal state.

According to the result of simulation, the sensitive load voltage THD is about 13% in this case, which is out of IEEE standards (less than 5%).

CASE ONE, SCENARIO B

For the second test electric spring should compensate voltage fluctuations without any source voltage harmonics with the PR controller so as a result of these tests Fig. 14 shows compensated sensitive load voltage. Fig. 14 shown that sensitive load voltage is stable in its reference value (311) and confirms the performance of the electric spring in the voltage fluctuations mode with proposed PR controller. As expected, the amplitude of voltage of the sensitive load remained constant at its reference value.

CASE ONE, SCENARIO C

For the third test electric spring should compensate voltage fluctuations and standard source voltage harmonics, order up to 17, without nonlinear load with the PR controller so as a result of these tests Fig. 15 shown compensated voltage. According to Fig. 15, which indicates the amplitude of the sensitive load voltage and also due to the sensitive load voltage THD that's equal to 1.3% its can be obtained that the performance of the electric spring in this situation with proposed PR controller will be approved.

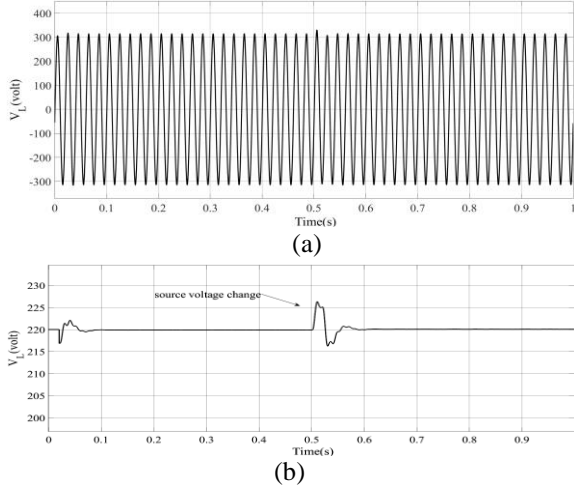


Figure 10. (a)Time waveform of sensitive load voltage (b) RMS waveform of sensitive load voltage

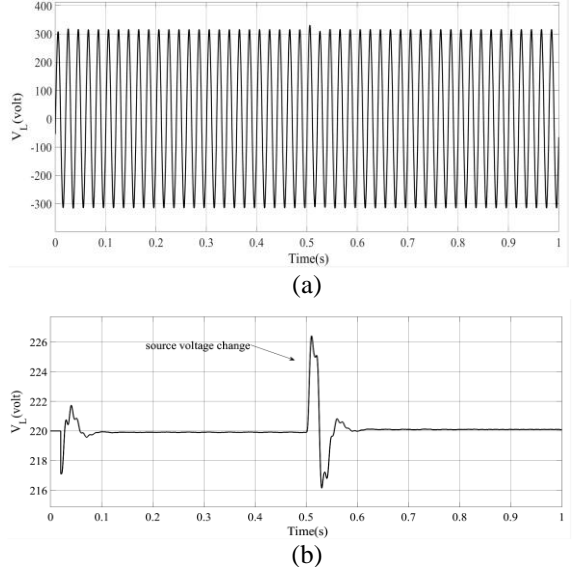


Figure 15. (a)Time waveform of sensitive load voltage (b) RMS waveform of sensitive load voltage

CASE ONE, SCENARIO D

For the fourth test electric spring should compensate voltage fluctuations with source voltage harmonics and nonlinear load parallel to sensitive load with the PR controller so as a result of these tests Fig. 16 and Fig.17 Respectively shown compensated voltage of sensitive load and electric spring output voltage:

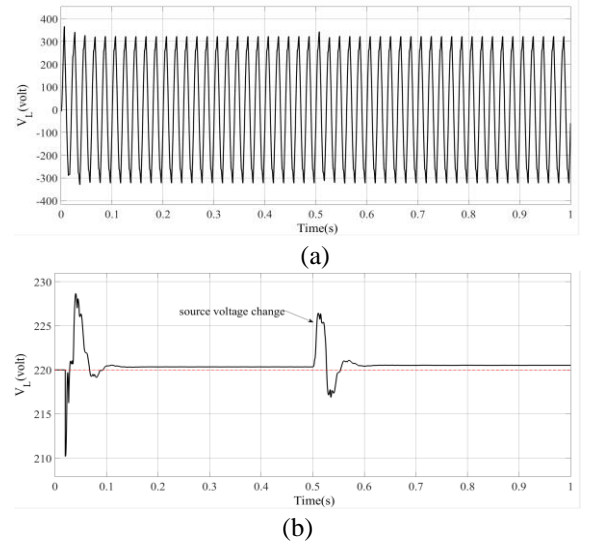


Figure 16. (a)Time waveform of sensitive load voltage (b) RMS waveform of sensitive load voltage

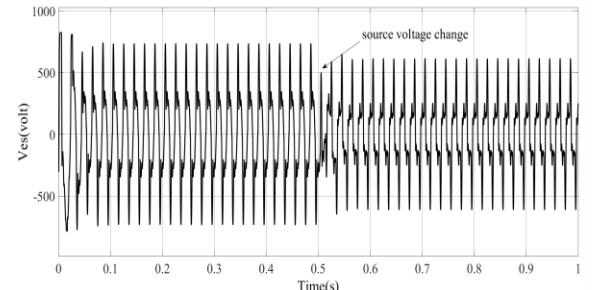


Figure 11. Single phase electric spring voltage

It can be seen from Fig. 16 the electric spring is operating good enough in voltage compensation and voltage error is about 0.3 volt but based on the simulation the THD value is not acceptable (this value must be below 5%) with proposed PR controller.

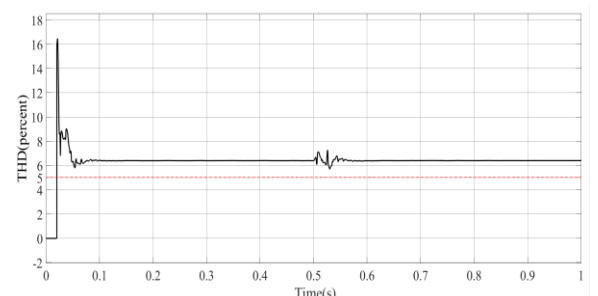


Figure 12. Sensitive load THD

As it can be seen from Fig.18, THD value is about 6.38% and not acceptable by IEEE standards but it has significantly decreased compared to the uncontrolled state.

CASE ONE, SCENARIO E

For the last test in single phase mode electric spring should compensate voltage fluctuations with source voltage harmonics and nonlinear load, with current characteristic as shown in Fig. 19, parallel to the sensitive load with the PR and RC controller so as a result of these tests Fig. 20 and Fig. 21 Respectively shown compensated voltage of sensitive load and Sensitive load THD:

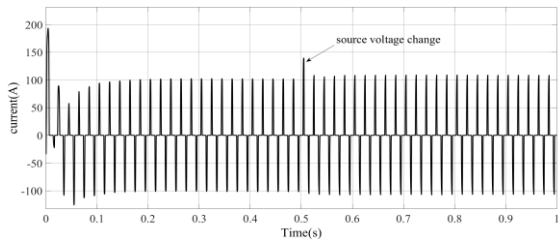
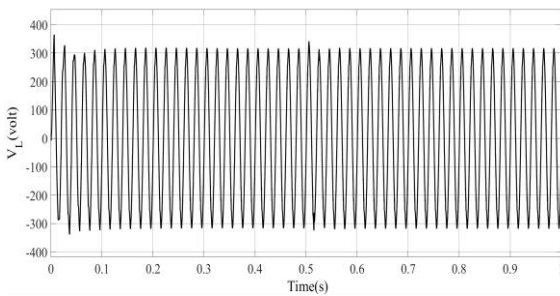
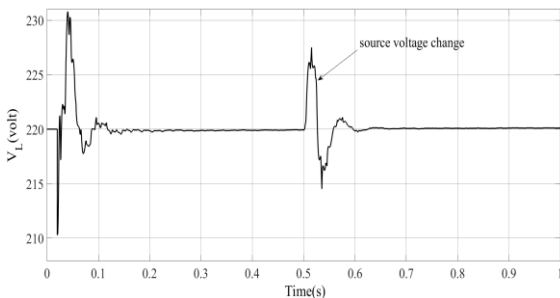


Figure 13. Current characteristic of the nonlinear load



(a)



(b)

Figure 20. (a)Time waveform of sensitive load voltage (b) RMS waveform of sensitive load voltage

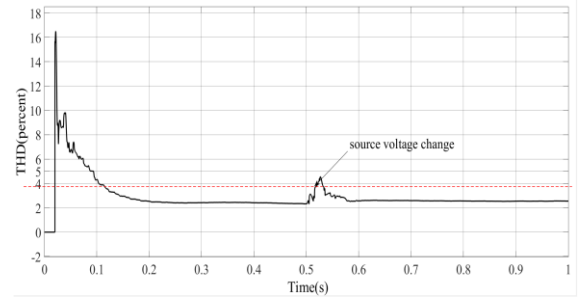


Figure 21. Sensitive load voltage THD

As it can be seen from Fig. 20 and Fig. 21 electric spring compensated voltage amplitude and works good enough to pass IEEE standard about THD. THD value with proposed controller is about 2.56% and decreased 59.87% Compared to the case study (D) and also by 80.31% compared to the non-controller state. Fig. 22 shows electric spring output voltage.

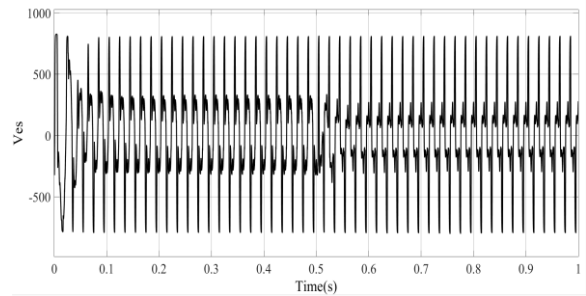


Figure 22. Single phase electric spring voltage

Fig. 23 shows the single-phase power factor in E case study, which has a non-linear load parallel to the sensitive load.

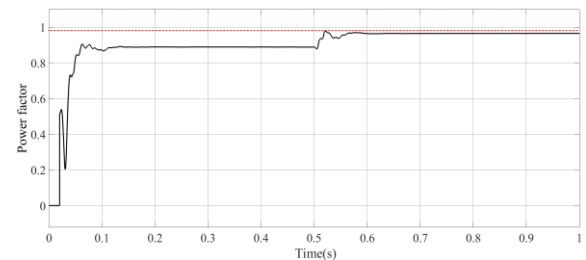


Figure 23. Single phase power factor

According to the Fig. 23 that shows the power factor value, it will be obtained that the power factor is close to the unit value.

5.2. Three Phase Load

CASE TWO, SCENARIO F

In this test, the 3-phase grid in state which the voltage of this grid has standard harmonics up to order 17, in addition to the decrease and increase in voltage magnitude and also a diode rectifier connected to phase (a) parallel to sensitive load and act as a nonlinear load (It should be noted that the

three-phase load used will not be a balanced anymore). Three phase loads connected to the grid with star structure and phase impedance is equal to 8Ω . Others grid parameter is same as table.2. Input voltage waveform is shown in Fig. 24.

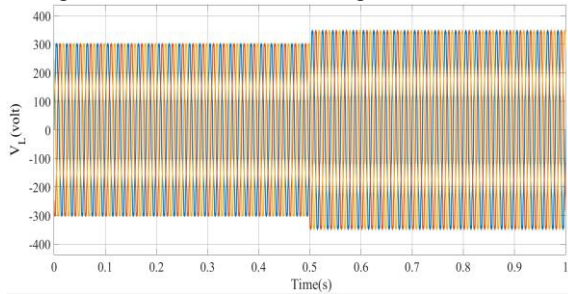


Figure 14. Three phase source voltage before compensation

Fig. 24 displays that the voltage amplitude fluctuates and also waveform goes out of sinusoidal state due to the presence of harmonics. The electric spring must be able to bring the waveform closer to the sinusoidal state and also bring the voltage amplitude to a reference value.

The three-phase voltage diagram of sensitive load after compensating through the electrical spring with designed controller (PR_RC) shows in Fig. 25.

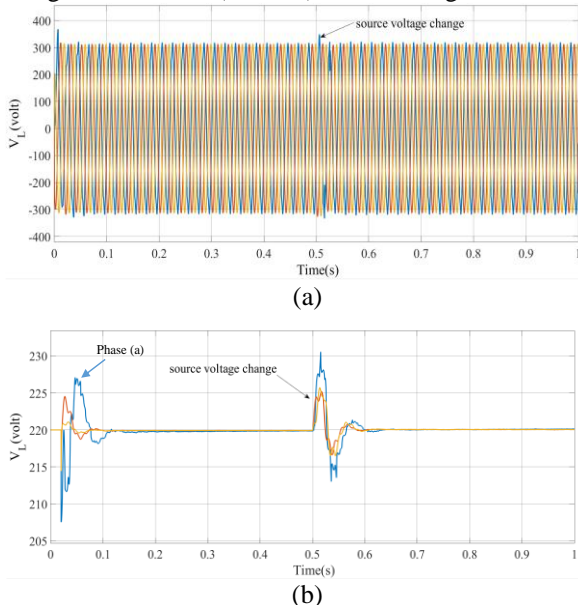


Figure 15. (a)Time waveform three phase load voltage after compensation(b)three phase RMS value of sensitive load voltage

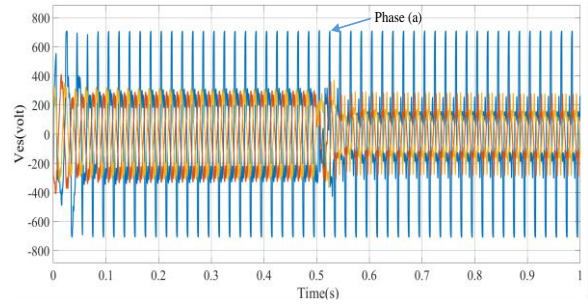


Figure 26. Three phase Ves

From Fig. 25 the three-phase voltage amplitude is fixed on 311 volt and waveforms are close to full sine wave state.

From simulation it is obtained that by using proposed PR_RC controller explained in this paper the three-phase voltage THD value is about 2.5% and pass the IEEE standards. The Three-phase power factor also is about 1 in this case study with the proposed controller. Figure 26 shows the electrical spring output voltage. The imbalance in the voltage level of the electrical spring is caused by the difference of the three-phase load (non-linear load in phase A).

Fig. 27 summarizes the results of the proposed methods.

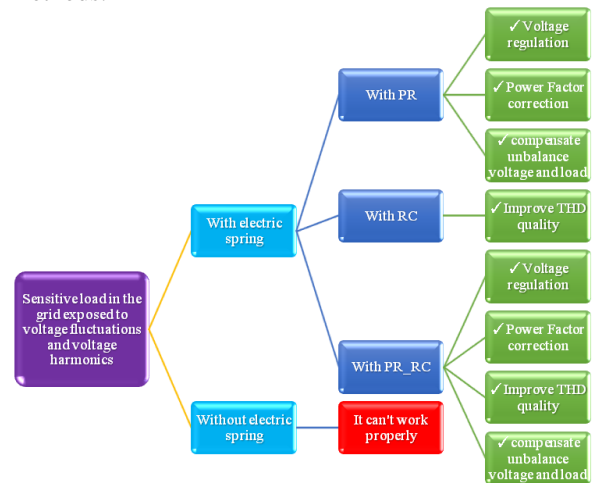


Figure 16. Summary of the results of the proposed methods

6. CONCLUSION

This article proposes a novel advanced control technique based on the proportional-resonant and repetitive controller for type II electric spring to Remove at the same time the total impact of grid voltage fluctuation, grid voltage harmonics, and nonlinear local load on the sensitive load voltage. by an overview of simulation results of the planned system in different working modes, can be seen that this controller will be able to completely Control the

sensitive load voltage at a steady amplitude and sinusoidal waveform; In situations where the grid voltage fluctuates and also included harmonics up to order 17 and local nonlinear load have raised the voltage harmonics. in the three-phase mode in addition to the issues of power quality mentioned in the single-phase grid, the three-phase load is unbalanced. according to simulations the THD value of the voltage decreased by 80.31 percent relative to the uncontrolled state and will be less than the value defined by the IEEE standard and the power factor will be very close to unit.

References

- [1] Q. Wang, W. Zuo, M. Cheng, F. Deng, and G. Buja, "Decoupled power control with in-depth analysis of single-phase electric springs," *IEEE Access*, vol. 8, pp. 21866–21874, 2020, doi: 10.1109/ACCESS.2020.2966677.
- [2] S. Y. Hui, C. K. Lee, and F. F. Wu, "Electric Springs—A New Smart Grid Technology," *IEEE Trans. Smart Grid*, vol. 3, no. 3, pp. 1552–1561, Sep. 2012, doi: 10.1109/TSG.2012.2200701.
- [3] S. H. C. Cherukuri, B. Saravanan, and K. S. Swarup, "A new control algorithm for energy conservation from main grid during generation intermittence in the micro grids using A.C electric springs," in *2016 21st Century Energy Needs - Materials, Systems and Applications (ICTFCEN)*, Nov. 2016, pp. 1–6, doi: 10.1109/ICTFCEN.2016.8052752.
- [4] E. F. Areed and M. A. Abido, "Design and dynamic analysis of Electric Spring for voltage regulation in smart grid," in *2015 18th International Conference on Intelligent System Application to Power Systems (ISAP)*, Sep. 2015, pp. 1–6, doi: 10.1109/ISAP.2015.7325565.
- [5] M. D. Solanki and S. K. Joshi, "Taxonomy of Electric springs: An enabling smart grid technology for effective demand side management," in *2015 Annual IEEE India Conference (INDICON)*, Dec. 2015, pp. 1–6, doi: 10.1109/INDICON.2015.7443227.
- [6] C. K. Lee, B. Chaudhuri, and S. Y. Hui, "Hardware and Control Implementation of Electric Springs for Stabilizing Future Smart Grid With Intermittent Renewable Energy Sources," *IEEE J. Emerg. Sel. Top. Power Electron.*, vol. 1, no. 1, pp. 18–27, Mar. 2013, doi: 10.1109/JESTPE.2013.2264091.
- [7] M.-H. Wang, T.-B. Yang, S.-C. Tan, and S. Y. Hui, "Hybrid Electric Springs for Grid-Tied Power Control and Storage Reduction in AC Microgrids," *IEEE Trans. Power Electron.*, vol. 34, no. 4, pp. 3214–3225, Apr. 2019, doi: 10.1109/TPEL.2018.2854569.
- [8] J. Soni and S. K. Panda, "Electric Spring for Voltage and Power Stability and Power Factor Correction," *IEEE Trans. Ind. Appl.*, vol. 53, no. 4, pp. 3871–3879, Jul. 2017, doi: 10.1109/TIA.2017.2681971.
- [9] S. Yan, M.-H. Wang, T.-B. Yang, S.-C. Tan, B. Chaudhuri, and S. Y. R. Hui, "Achieving Multiple Functions of Three-Phase Electric Springs in Unbalanced Three-Phase Power Systems Using the Instantaneous Power Theory," *IEEE Trans. Power Electron.*, vol. 33, no. 7, pp. 5784–5795, Jul. 2018, doi: 10.1109/TPEL.2017.2748221.
- [10] C. K. Lee, N. R. Chaudhuri, B. Chaudhuri, and S. Y. R. Hui, "Droop Control of Distributed Electric Springs for Stabilizing Future Power Grid," *IEEE Trans. Smart Grid*, vol. 4, no. 3, pp. 1558–1566, Sep. 2013, doi: 10.1109/TSG.2013.2258949.
- [11] N. Tang, K. Yang, H. Huang, and C.-K. Lee, "The Application of One-Cycle Control Technology in Electric Spring System," *IOP Conf. Ser. Earth Environ. Sci.*, vol. 170, no. 4, p. 042117, Jul. 2018, doi: 10.1088/1755-1315/170/4/042117.
- [12] Y. Zou, M. Z. Q. Chen, Y. Hu, and Y. Zou, "Steady-State Analysis and Output Voltage Minimization Based Control Strategy for Electric Springs in the Smart Grid with Multiple Renewable Energy Sources," *Complexity*, vol. 2019, 2019, doi: 10.1155/2019/5376360.
- [13] K.-T. Mok, S.-C. Tan, and S. Y. R. Hui, "Decoupled Power Angle and Voltage Control of Electric Springs," *IEEE Trans. Power Electron.*, vol. 31, no. 2, pp. 1216–1229, Feb. 2016, doi: 10.1109/TPEL.2015.2424153.
- [14] S. Tan, C. K. Lee, and S. Y. Hui, "General Steady-State Analysis and Control Principle of Electric Springs with Active and Reactive Power Compensations," *IEEE Trans. Power Electron.*, vol. 28, no. 8, pp. 3958–3969, 2013, doi: 10.1109/TPEL.2012.2227823.
- [15] Q. Wang, M. Cheng, Z. Chen, and Z. Wang, "Steady-State Analysis of Electric Springs with a Novel δ Control," *IEEE Trans. Power Electron.*, vol. 30, no. 12, pp. 7159–7169, 2015, doi: 10.1109/TPEL.2015.2391278.
- [16] Q. Wang, M. Cheng, Y. Jiang, W. Zuo, and G. Buja, "A Simple Active and Reactive Power Control for Applications of Single-Phase Electric Springs," *IEEE Trans. Ind. Electron.*, vol. 65, no. 8, pp. 6291–6300, Aug. 2018, doi: 10.1109/TIE.2018.2793201.

- [17] E. F. Areed, M. A. Abido, A. T. Al-Awami, and S. A. Hussain, "Electric spring average model development and dynamic analysis for demand-side management," *IET Smart Grid*, vol. 3, no. 2, pp. 226–236, 2020, doi: 10.1049/iet-stg.2018.0149.
- [18] Q. Wang, Z. Ding, M. Cheng, F. Deng, and G. Buja, "A Parameter-Exempted, High-Performance Power Decoupling Control of Single-Phase Electric Springs," *IEEE Access*, vol. 8, pp. 33370–33379, 2020, doi: 10.1109/ACCESS.2020.2972917.
- [19] D. Zammit, C. Spiteri Staines, M. Apap, and J. Licari, "Design of PR current control with selective harmonic compensators using Matlab," *J. Electr. Syst. Inf. Technol.*, vol. 4, no. 3, pp. 347–358, Dec. 2017, doi: 10.1016/j.jesit.2017.01.003.
- [20] Y. Yang, K. Zhou, and F. Blaabjerg, "Frequency adaptability of harmonics controllers for grid-interfaced converters," *Int. J. Control*, vol. 90, no. 1, pp. 3–14, Jan. 2017, doi: 10.1080/00207179.2015.1022957.
- [21] Q.-N. Trinh and H.-H. Lee, "An Enhanced Grid Current Compensator for Grid-Connected Distributed Generation Under Nonlinear Loads and Grid Voltage Distortions," *IEEE Trans. Ind. Electron.*, vol. 61, no. 12, pp. 6528–6537, Dec. 2014, doi: 10.1109/TIE.2014.2320218.
- [22] M. Steinbuch, "Repetitive control for systems with uncertain period-time," *Automatica*, vol. 38, no. 12, pp. 2103–2109, Dec. 2002, doi: 10.1016/S0005-1098(02)00134-6.
- [23] Y. Yuan, F. Auger, L. Loron, S. Moisy, and M. Hubert, "Overshootless repetitive control," in *2015 IEEE 24th International Symposium on Industrial Electronics (ISIE)*, Jun. 2015, vol. 2015-Septe, no. June, pp. 106–112, doi: 10.1109/ISIE.2015.7281452.